Semiannual oscillations in the atmosphere of Mars

Takeshi Kuroda,[1] Alexander S. Medvedev,[2] Paul Hartogh,[2] and Masaaki Takahashi[3]

Received 18 September 2008; accepted 29 October 2008; published 4 December 2008.

[1] We report on the first detection of the semiannual oscillation (SAO) in the Martian atmosphere. The semiannual periodicity is found in the difference between day- and night-time atmospheric temperatures, a good proxy for solar tides, measured from Mars Global Surveyor. Simulations with a general circulation model proved that this modulation of tidal amplitudes is a manifestation of the SAO of zonal winds in Martian tropics. Our numerical experiments revealed significant differences in driving mechanisms of the SAO between Mars and Earth. On Mars, unlike on Earth, equatorial Kelvin waves supply only small retrograde torque to the mean circulation. Instead, thermal tides and quasi-stationary planetary waves induced by Martian topography contribute strongly to the prograde (super-rotation) acceleration. The existence of the SAO on Mars suggests that this phenomenon is not a result of the unique terrestrial environment, but a more general consequence of wave-mean flow interactions in atmospheres of fast-rotating planets. **Citation:** Kuroda, T., A. S. Medvedev, P. Hartogh, and M. Takahashi (2008), Semiannual oscillations in the atmosphere of Mars, *Geophys. Res. Lett.*, *35*, L23202, doi:10.1029/2008GL036061.

1. Introduction

[2] The semiannual oscillation (SAO) of the mean zonal wind in tropics is a prominent feature of the upper stratosphere and mesosphere of Earth. A number of observational studies have documented the terrestrial SAO [*Garcia et al.*, 1997; *Burrage et al.*, 1996]. Although the alternation of westerly (prograde) and easterly (retrograde) winds in low latitudes is apparently concomitant with the annual radiative cycle (the sun crosses the equator twice a year), the SAO is driven dynamically. Axisymmetric cross-equatorial transport associated with the thermally induced circulation maintains easterly winds over the equator [*Holton and Wehrbein*, 1980]. In order to explain the acceleration of air parcels to a super-rotation with respect to the surface during westerly phases of the SAO, non-axisymmetric effects must be invoked.

[3] The role of eddies in forcing the terrestrial SAO was extensively studied. *Dunkerton* [1979] showed that large-scale Kelvin waves propagating from below induce westerly winds in the stratosphere. Planetary Rossby waves traveling from mid-latitudes of the winter hemisphere contribute to the easterly acceleration [*Hamilton*, 1986; *Ray et al.*, 1998]. Vertically propagating gravity waves filtered by the stratospheric SAO supply the momentum to drive both westerly and easterly winds in the mesosphere [*Dunkerton*, 1982; *Medvedev and Klaassen*, 2001]. General circulation models (GCMs) have been applied to simulate the SAO [e.g., *Sassi et al.*, 1993]. At present, GCMs extending from the surface up to 100–150 km reproduced the stratospheric and mesospheric SAO consistently with observations, and helped to clarify the driving mechanism of the terrestrial SAO [*Medvedev and Klaassen*, 2001; *Richter and Garcia*, 2006]. In this paper we present the discovery of the SAO on Mars and the study of its forcing using a Martian GCM.

2. SAO Signal in the MGS-TES Data

[4] To date, there are virtually no measurements of the equatorial wind on Mars except for some sparse data with very low resolution [e.g., *Clancy et al.*, 2006]. In mid- and high latitudes, the wind can be estimated from numerous temperature profiles acquired with the Martian orbiters using the so-called thermal wind relation, as, for instance, was done for the Thermal Emission Spectrometer aboard Mars Global Surveyor (MGS-TES) [e.g., *Smith et al.*, 2001]. Unfortunately, this relation breaks down and is of little use in low latitudes.

[5] On the other hand, the background zonal wind strongly affects the propagation of solar tides [*Lindzen and Hong*, 1974], and even controls to a large degree the seasonal variability of the diurnal tide in the atmosphere of Earth [*Achatz et al.*, 2008]. Substantial effects of the solstitial mean zonal wind on the tide propagation were found on Mars [*Wilson and Hamilton*, 1996]. Therefore, if the SAO in the Martian atmosphere exists, the seasonally varying tropical wind must necessarily modulate the propagation of solar tides. Following this assumption, we analyzed the temperature difference between the day- (local time ~2:00 pm) and night-time (local time ~2:00 am) retrieved from the MGS-TES limb measurements during Mars Years 24 and 25 (MY24-25). The absolute value of this difference provides a good measure of twice the amplitude of the diurnal sun-synchronous tide [*Banfield et al.*, 2003]. Figure 1a shows a clear semiannual signal between 0.5 and 0.05 mb (approximately 25–50 km) with the peak values $\Delta T \sim 6$–8 K near the equinoxes (the solar longitudes L_s = 0 and 180°) and minima around the solstices (L_s = 90 and 270°).

3. Simulation of the Martian SAO Using a General Circulation Model

[6] To find out if the observed tidal signature is really caused by the SAO, we applied our Martian general circulation model (MGCM) [*Kuroda et al.*, 2005] to simulate long period variations of the tropical wind. The model

[1] Institute of Space and Astronautical Science, Japan Aerospace Exploration Agency, Sagamihara, Japan.
[2] Max Planck Institute for Solar System Research, Katlenburg-Lindau, Germany.
[3] Center for Climate System Research, University of Tokyo, Kashiwa, Japan.

0094-8276/08/2008GL036061$05.00

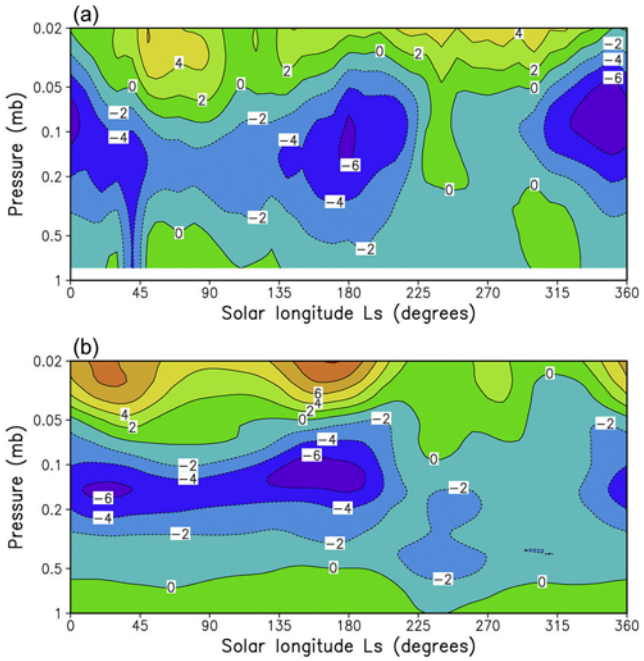

Figure 1. (a) Seasonal change of the temperature difference between local day and night divided by 2, $(T_{2PM}\text{-}T_{2AM})/2$, averaged between 10°S and 10°N from the MGS-TES limb observations. The data in this plot are for the period from L_s = 125° in Mars Year 24 (April 1999) to L_s = 125° in Mars Year 25 (March 2001). The contour interval is 2 K. (b) Same as Figure 1a but from the CCSR/NIES MGCM run with the seasonally varying dust opacity (TES2 scenario) corresponding to the period of observations in Figure 1a.

is based on the CCSR/NIES (Center for Climate System Research/National Institute of Environmental Studies, Japan) terrestrial GCM [*Numaguti et al.*, 1995], utilizes a spectral solver for the three-dimensional primitive equations, and has a comprehensive suite of physical parameterizations for the Martian atmosphere [*Kuroda et al.*, 2005]. The model accounts for the realistic topography, albedo and thermal inertia on the surface, and for the CO_2 condensation/sublimation including the change of the air mass and the surface CO_2 snow cover. It computes the radiative effects of carbon dioxide (under the local thermodynamic equilibrium) and of airborne dust in the solar and infrared wavelengths. The model has been validated against the existing measurements on Mars including the zonal mean climatology [*Kuroda et al.*, 2005], baroclinic planetary waves [*Kuroda et al.*, 2007] and zonal-mean variability in mid- and high-latitudes [*Yamashita et al.*, 2007]. The vertical grid has 30 σ-levels with the model lid at ~80 km, and the horizontal resolution is set to about 5.6° × 5.6° (~333 km at the equator).

[7] The simulations were carried out for 7 model Martian years starting with the initial isothermal and windless state, and the output from the last 5 years was used for the analysis in the form of composite cycles. To match the meteorological conditions of the MY24-25, we prescribed the seasonal and latitudinal variations of the dust opacity in accordance with the MGS-TES retrievals during the same time (TES2 dust scenario by *Kuroda et al.* [2005]). This was a period with a "minor" dust storm during the southern spring with the increased dust opacity in the visible wavelength ~0.7–1.5, and ~0.2 in other seasons. The simulated seasonal change of the temperature difference at 2 pm and 2 am of local time over the equator in Figure 1b shows a remarkable agreement with the observations in Figure 1a including the semiannual signal around 0.1–0.3 mb.

[8] Indeed, the modeled annual cycle of the mean zonal wind averaged between 10°S and 10°N (Figure 2a) demonstrates a clear SAO with alternating westerlies (superrotation, prograde wind) in equinoxes and easterlies (retrograde wind) in solstices between 0.2–1 mb (~20–35 km). Its phase is similar to the stratospheric SAO on Earth [*Garcia et al.*, 1997; *Medvedev and Klaassen*, 2001], but an unexpectedly large seasonal asymmetry is seen between the northern (~−30 m s^{-1}) and southern (~−120 m s^{-1}) summers. Partly, it is related to the occurrence of the dust storm. When the run was repeated with the seasonally and spatially uniform dust opacity ~0.2 in the visible wavelength (Figure 2b), the

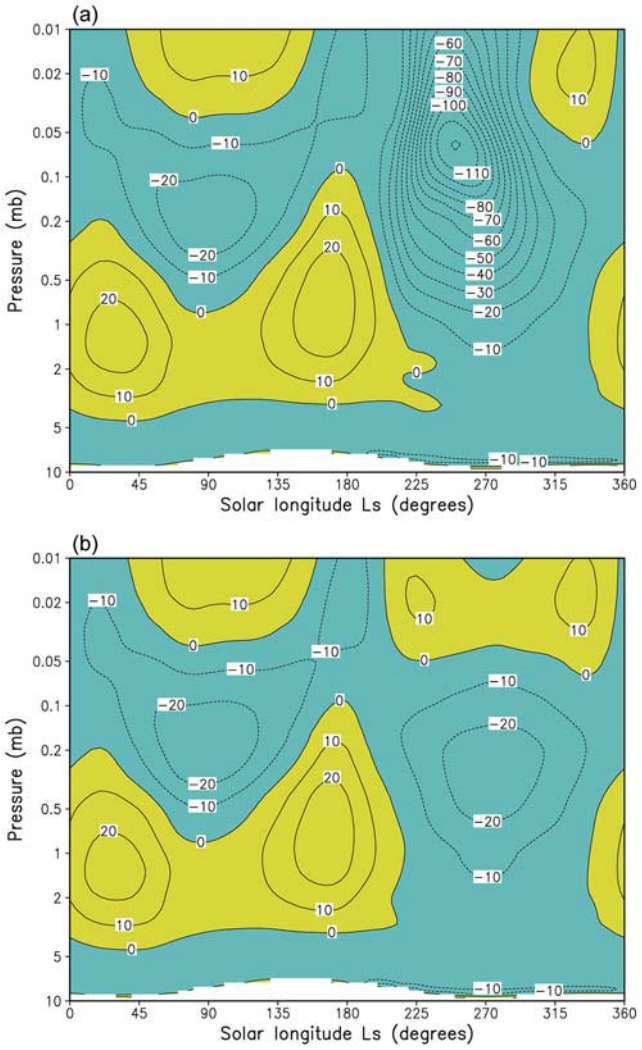

Figure 2. (a) The composite annual cycle of the simulated mean zonal wind averaged between 10°S and 10°N from the run with TES2 dust scenario. The contour interval is 10 m s^{-1}, westerly wind is shaded with yellow. (b) Same as Figure 2a, except from the run with the seasonally uniform dust opacity ~0.2.

magnitudes of the wind in both solstices became approximately equal, and the phase reversal above ~0.05 mb (~45 km) turned out to be more reminiscent of the terrestrial mesospheric SAO [*Garcia et al.*, 1997; *Richter and Garcia*, 2006]. Nevertheless, some seasonal asymmetry (westerly wind at 1–4 mb during northern summer solstices and easterlies below ~0.05 mb in southern summers) remains and, thus, requires some explanation.

[9] The run with the circular Martian orbit yielded little difference in the wind distribution suggesting that the eccentricity of the orbit plays no role in the seasonal asymmetry of the SAO. However, a remarkable change occurred when we replaced the real topography with the flat surface: the asymmetry strongly diminished, and the westerly phase almost disappeared. Apparently, the SAO is closely related to the strength of the meridional Hadley circulation, which, in turn, is determined by the zonally-averaged cross-equatorial topographic slope [*Richardson and Wilson*, 2002].

4. Driving Mechanism of the Martian SAO

[10] What causes the acceleration of air parcels to global super-rotation with respect to the surface during westerly phases of the SAO? To investigate the forcing of the Martian SAO, we use the horizontal momentum equation in the transformed Eulerian mean (TEM) formalism [*Andrews et al.*, 1987]:

$$\frac{\partial \overline{u}}{\partial t} = \overline{v}^* \left[f - \frac{(\overline{u}\cos\phi)_\phi}{a\cos\phi} \right] - \overline{w}^* \overline{u}_z + \frac{\nabla \cdot \mathbf{F}}{\rho_0 a \cos\phi} + \overline{X}, \qquad (1)$$

where $\overline{u}$ is the mean zonal wind, (0, $\overline{v}^*$, $\overline{w}^*$) is the residual mean meridional circulation, overbars denote zonal averaging, f is the Coriolis parameter, a is the radius of Mars, ϕ is the latitude, $\mathbf{F}$ is the Eliassen-Palm (EP) flux due to non-zonal eddies, ρ_0 is the atmospheric reference density, and $\overline{X}$ is the parameterized (subgrid) forcing. The latter describes the effects of the sponge layer near the top of the model, horizontal and vertical diffusion, and indirect effects of the convective adjustment. Mean zonal torque supplied by the meridional and vertical advection, and eddies was calculated from the first, second and third terms of the right-hand part of (1), respectively. The term containing the Coriolis parameter, although small near the equator, was formally included in the meridional advection.

[11] Figure 3 presents the averaged between 10°S and 10°N forcing (global zonal wind acceleration) produced by the advection and eddies in the run with the uniform dust opacity ~0.2 (corresponding to the results in Figure 2b), as well as the total EP flux divergence due to all resolved waves. To evaluate the impact of various harmonics, we performed the temporal and spatial (in zonal direction) Fourier analysis of the 3-hourly model output and, subsequently, calculated the momentum deposition rate associated with each spectral component with periods ≥6 hours and zonal wavenumbers from 1 to 10. We found that only three types of non-zonal disturbances contribute appreciably to the acceleration. They are 1) quasi-stationary planetary waves with periods longer than 30 sols (Martian days), 2) westward-propagating diurnal-period harmonics associated with the thermal tide, and 3) eastward-traveling diurnal-period Kelvin waves [*Wilson*, 2000].

[12] As in the atmosphere of Earth [*Holton and Wehrbein*, 1980], the meridional advection supplies mainly the easterly (retrograde) momentum, especially in solstices when the cross-equatorial circulation exists (Figure 3a). Since f is negligible near the equator, the forcing due to the meridional advection is mostly proportional to the product of $\overline{v}^*$ and $\overline{u}_y$ (where dy = a dϕ). Both $\overline{v}^*$ and $\overline{u}_y$ are negative in northern summer solstice, and both are positive in northern winter one, which results in the easterly torque in both solstices. In equinoxes, the absolute values of both $\overline{v}^*$ and $\overline{u}_y$ are much smaller.

[13] In the simulation with the varying dust opacity (TES2 dust scenario by *Kuroda et al.* [2005]), the corresponding easterly forcing increases to -35 m s^{-1} sol^{-1} during dust storms around L_s = 240. The magnitude of the torque is larger during southern summers when the cross-equatorial transport is stronger, especially below ~0.5 mb, due to the global north-south elevation of the Martian topography [*Richardson and Wilson*, 2002]. The vertical advection contributes mainly to the westerly (prograde) wind acceleration (Figure 3b). It occurs due to the enhancement of the upward flow over the equator as well as due to the negative vertical wind shear. When we turned solar tides in the model off by replacing the diurnally varying insolation with its daily mean, the vertical advection became weaker, as did the associated SAO forcing, especially in equinoxes.

[14] The total wind forcing by waves (Figure 3c) shows that eddies provide mostly westerly momentum below 0.5 mb that does not display the semiannual cycle. In contrast, the eddy forcing has a clear semidiurnal variation above 0.5 mb. The momentum supplied by stationary planetary waves is mostly opposite to that by the meridional advection. These waves are induced by the flow over topography with a distinct zonal-wavenumber 2 structure at the equator. They produce strong westerly torque to the mean flow, especially during southern summers in the lower atmosphere (Figure 3d). This is opposite to the role of planetary Rossby waves on Earth, which transport the easterly momentum from the winter midlatitudes to the equator [*Hamilton*, 1986; *Ray et al.*, 1998].

[15] As seen in the MGS-TES data (Figure 1a) and well captured in our simulations (Figure 1b), the westward-moving tropical tide has large amplitudes in equinoxes. The associated forcing shows a clear semiannual structure (Figure 3e). The tide propagates upward from the surface providing the westerly momentum to the tropical wind within the region of thermal excitation through the mechanism outlined by *Fels and Lindzen* [1974]. In northern summers, it dissipates around ~0.2 mb, somewhat lower (~0.5 mb) in southern summers, and deposits the easterly momentum above these altitudes. Together with the vertical advection, the diurnal sun-synchronous tide is the main driver of the prograde phase of the SAO during equinoxes.

[16] Eastward propagating Kelvin waves produce weak easterly acceleration throughout all seasons and at all heights (Figure 3f). This is quite different from Earth, where Kelvin waves are excited by the equatorial moist convection in the troposphere, break higher, and strongly contribute to the westerly phase of the SAO [*Dunkerton*, 1979; *Sassi and Garcia*, 1997]. Note that the diurnal Kelvin wave with zonal wave 1 and 2 in the Mars atmosphere is

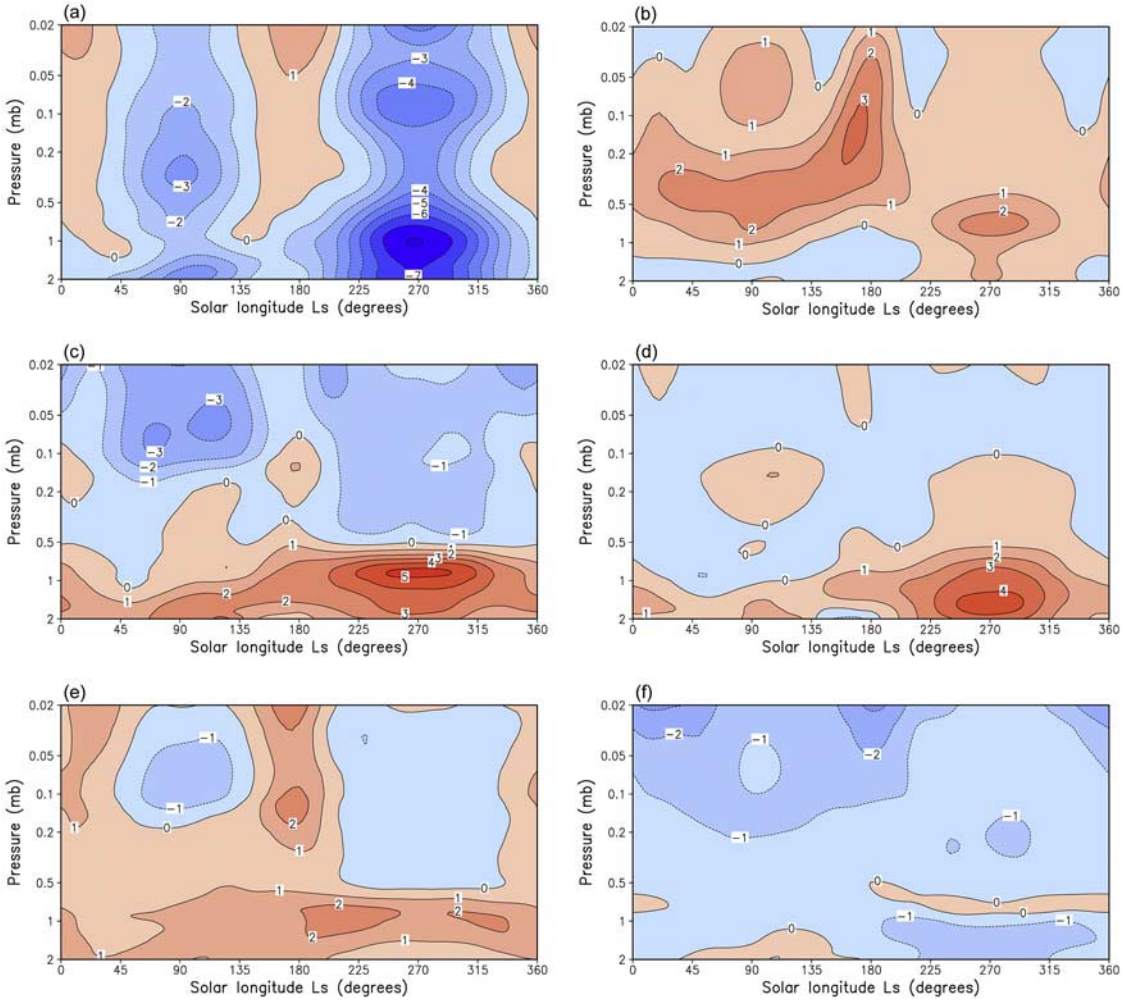

Figure 3. The composite annual cycle of the forcing: (a) by the meridional advection, (b) vertical advection, (c) total wave forcing, (d) quasi-stationary planetary waves, (e) westward-propagating diurnal-period waves (tides), and (f) eastward-propagating diurnal-period Kelvin waves from the run with the seasonally uniform dust opacity ~0.2. The contribution of harmonics with zonal wavenumbers 1–10 was added, and averaged between 10°S and 10°N. The contour interval is 1 m s^{-1} sol^{-1}, and the red shading denotes the prograde acceleration.

forced by interactions of the migrating diurnal tide with zonal wave 2 and 3 components of topography, respectively, and has an equivalent barotropic vertical structure, while its terrestrial counterparts possess a broad spectrum of phase velocities and vertical wavelengths.

5. Conclusions

[17] The discovered Martian SAO is reminiscent of the terrestrial one. This atmospheric phenomenon on both planets is a manifestation of wave-mean flow interactions, but the details of its forcing differ in many respects. Contrary to Earth, thermal tides play a significant role in maintaining the Martian SAO by supplying westerly forcing in equinoxes. The horizontal cross-equatorial transport associated with the Hadley circulation, which is sensitive to the topography and dust opacity, provides mainly the easterly torque to the equatorial mean zonal wind at solstices. The vertical advection due the rising air supplies mostly westerly (pro-grade) momentum. The contribution of vertical advection becomes weaker when tides are turned off in the simulations. This indicates that tides contribute to the super-rotation both directly and indirectly by affecting the residual circulation. In the lower atmosphere, quasi-stationary planetary waves generated by the flow over topography provide strong westerly momentum, in addition to tides. Unlike on Earth, effects of transient planetary waves excited by the baroclinic instability in midlatitudes are negligible for the wind forcing in tropics. Due to the lack of strong convective wave generation in Martian tropics, eastward-propagating diurnal-period Kelvin waves produce weak easterly acceleration at all seasons and all heights. This is quite different from Earth, where Kelvin waves are a major driving factor of the SAO.

[18] The found SAO signature in the equatorial atmosphere of Mars as well as our diagnostics using the GCM indicate that the SAO is not a result of peculiar terrestrial conditions, but an ubiquitous atmospheric phenomenon of fast-rotating planets. Recent detection of the SAO in the Saturn's atmosphere [*Orton et al.*, 2008], which was published after this manuscript was prepared, provides a strong argument in favor of the latter conclusion.

[19] **Acknowledgments.** The authors are grateful to Michael D. Smith of NASA for providing the MGS-TES observational data. Helpful com-

ments of John Wilson of GFDL and the anonymous reviewer helped to improve the presentation. This work was supported by German Research Foundation (DFG), grant HA 3261/3.

References

Achatz, U., N. Grieger, and H. Schmidt (2008), Mechanisms controlling the diurnal solar tide: Analysis using a GCM and a linear model, *J. Geophys. Res.*, *113*, A08303, doi:10.1029/2007JA012967.

Andrews, D. G., J. R. Holton, and C. B. Leovy (1987), *Middle Atmosphere Dynamics*, *Int. Geophys. Ser.*, vol. 40, edited by R. Dmowska and J. R. Holton, 489 pp, Academic, Orlando, Fla.

Banfield, D., B. J. Conrath, M. D. Smith, P. R. Christensen, and R. J. Wilson (2003), Forced waves in the Martian atmosphere from MGS TES nadir data, *Icarus*, *161*, 319–345.

Burrage, M. D., R. A. Vincent, H. G. Mayr, W. R. Skinner, N. F. Arnold, and P. B. Hays (1996), Long-term variability in the equatorial middle atmosphere zonal wind, *J. Geophys. Res.*, *101*, 12,847–12,854.

Clancy, R. T., B. J. Sandor, G. H. Moriarty-Schieven, and M. D. Smith (2006), Mesosphelic winds and temperatures from JCMT sub-millimeter CO line observations during the 2003 and 2005 Mars oppositions, in *Second Workshop on Mars Atmosphere Modeling and Observations*, edited by F. Forget et al., 134–138, LMD, IAA, AOPP, CNES and ESA, Granada, Spain.

Dunkerton, T. (1979), On the role of the Kelvin wave in the westerly phase of the semiannual zonal wind oscillation, *J. Atmos. Sci.*, *36*, 32–41.

Dunkerton, T. J. (1982), Theory of the mesopause semiannual oscillation, *J. Atmos. Sci.*, *39*, 2681–2690.

Fels, S. B., and R. S. Lindzen (1974), The interaction of thermally excited gravity waves with mean flows, *Geophys. Fluid Dyn.*, *6*, 149–191.

Garcia, R. R., T. J. Dunkerton, R. S. Lieberman, and R. A. Vincent (1997), Climatology of the semiannual oscillation of the tropical middle atmosphere, *J. Geophys. Res.*, *102*, 26,019–26,032.

Hamilton, K. P. (1986), Dynamics of the stratospheric semiannual oscillation, *J. Meteorol. Soc. Jpn.*, *64*, 227–244.

Holton, J. R., and W. M. Wehrbein (1980), A numerical model of the zonal mean circulation of the middle atmosphere, *Pure Appl. Geophys.*, *118*, 284–306.

Kuroda, T., N. Hashimoto, D. Sakai, and M. Takahashi (2005), Simulation of the Martian atmosphere using a CCSR/NIES AGCM, *J. Meteorol. Soc. Jpn.*, *83*, 1–19.

Kuroda, T., A. S. Medvedev, P. Hartogh, and M. Takahashi (2007), Seasonal change of the baroclinic wave activity in the northern hemisphere of Mars simulated with a GCM, *Geophys. Res. Lett.*, *34*, L09203, doi:10.1029/2006GL028816.

Lindzen, R. S., and S. S. Hong (1974), Effects of mean winds and horizontal temperature gradients on solar and lunar semidiurnal tides in the atmosphere, *J. Atmos. Sci.*, *31*, 1421–1466.

Medvedev, A. S., and G. P. Klaassen (2001), Realistic semiannual oscillation simulated in a middle atmosphere general circulation model, *Geophys. Res. Lett.*, *28*, 733–736.

Numaguti, A., M. Takahashi, T. Nakajima, and A. Sumi (1995), Development of atmospheric general circulation model, in *Climate System Dynamics and Modeling*, edited by T. Matsuno, pp. 1–27, Cent. for Clim. Syst. Res., Univ. of Tokyo, Tokyo.

Orton, G. S., et al. (2008), Semi-annual oscillations in Saturn's low-latitude stratospheric temperatures, *Nature*, *453*, 196–199.

Ray, E. A., M. J. Alexander, and J. R. Holton (1998), An analysis of the structure and forcing of the equatorial semiannual oscillation in zonal wind, *J. Geophys. Res.*, *103*, 1759–1774.

Richardson, M. I., and R. J. Wilson (2002), A topographically forced asymmetry in the Martian circulation and climate, *Nature*, *416*, 298–301.

Richter, J. H., and R. R. Garcia (2006), On the forcing of the mesospheric semi-annual oscillation in the Whole Atmosphere Community Climate Model, *Geophys. Res. Lett.*, *33*, L01806, doi:10.1029/2005GL024378.

Sassi, F., and R. R. Garcia (1997), The role of equatorial waves forced by convection in the tropical semiannual oscillation, *J. Atmos. Sci.*, *54*, 1925–1942.

Sassi, F., R. R. Garcia, and B. A. Boville (1993), The stratospheric semiannual oscillation in the NCAR community climate model, *J. Atmos. Sci.*, *50*, 3608–3624.

Smith, M. D., J. C. Pearl, B. J. Conrath, and P. R. Christensen (2001), Thermal Emission Spectrometer results: Mars atmospheric thermal structure and aerosol distribution, *J. Geophys. Res.*, *106*, 23,929–23,945.

Wilson, J., and K. Hamilton (1996), Comprehensive model simulation of thermal tides in the Martian atmosphere, *J. Atmos. Sci.*, *53*, 1290–1326.

Wilson, R. J. (2000), Evidence for diurnal period Kelvin waves in the Martian atmosphere from Mars Global Surveyor TES data, *Geophys. Res. Lett.*, *27*, 3889–3892.

Yamashita, Y., T. Kuroda, and M. Takahashi (2007), Maintenance of zonal wind variability associated with the annular mode on Mars, *Geophys. Res. Lett.*, *34*, L16819, doi:10.1029/2007GL030069.

P. Hartogh and A. S. Medvedev, Max Planck Institute for Solar System Research, D-37191 Katlenburg-Lindau, Germany.

T. Kuroda, Institute of Space and Astronautical Science, Japan Aerospace Exploration Agency, 3-1-1 Yoshinodai, Sagamihara, Kanagawa, 229-8510, Japan. (kuroda@isas.jaxa.jp)

M. Takahashi, Center for Climate System Research, University of Tokyo, 5-1-5 Kashiwanoha, Kashiwa, Chiba, 277-8568, Japan.